Ceramics International **24** (1998) 359–364

PII: S0272-8842(97)00022-9
0272-8842/98 $19.00+.00

Finite Element Simulation of Vickers Microindentation on Alumina Ceramics

Tadeusz Niezgoda* & Jerzy Małachowski
Military University of Technology, Kaliskiego 2, 01-489 Warsaw, Poland

Marek Boniecki
Institute of Electronic Materials Technology, Wólczyńska 133, 01-919 Warsaw, Poland

(Received 17 June 1996; accepted 17 February 1997)

Abstract: A three-dimensional finite element method was applied to simulation of the microindentation process in Al_2O_3 ceramics. This simulation was based on the elastic theory of material deformation. The crushing criterion in numerical solution was based on energy value obtained from the stress state. The energy value was compared with the work of the indenter. The calculations provided distribution and residual equivalent stresses during and after the indentation test.

1 INTRODUCTION

The computer simulation of physical processes is one of the present directions of research and development of bodies and structures behaviour. The achieved method (experimentally confirmed) gives an opportunity to analyse the same problems numerically, without experiment, which are often expensive.

Many research groups[1,2] apply the numerical methods to analyse such problems as: creating and the growing of cracks and structure collapse.

For the last few years the finite element method (FEM)[3,4] has often been used to investigate the above problems[5–7]. For the elastic materials the main matrix equation can be written as follows:

$$KU_i = P_i \tag{1}$$

where K is the stiffness matrix, which depends on geometry and materials properties, U_i is the unknown nodal displacements vector and P_i is force loading vector.

Solving eqn (1) and calculating U_i vector allows to calculate strains and stresses in the given body. The advantage of the FEM calculations is the possibility of using in the same finite element mesh tor different vectors P_i (loading force) and different boundary conditions.

*To whom correspondence should be addressed.

The authors of the papers[7] used the FEM for calculating the deformation and stress state for elastic-plastic materials during the Vickers indentation test on coated systems.

The microindentation test allows measuring the amount of force required to push rigid indenter on a given distance into a material. Hardness formally defined from the quotient force value (action on indenter) and depth indentate can be calculated from the experiment.

The crack calculation parameters shown allow to define the stress intensity factor K_{IC}[8,9] There are numerous defined formulas of the factor for the Vickers indentation test.[10,11]

The authors of this paper consider that the equivalent stress state in the ceramic appears due to motion of the indenter in numerical simulation. The stress state can cause local crushing and cracking in the material. It was assumed that the ceramics are brittle and elastic.[12]

The aim of the paper was to propose the method of numerical simulation of the indentation process.

2 EXPERIMENT

Experiment was performed by Vickers indentation on Al_2O_3 ceramic material on Zwick testing machine. The alumina ceramics in the experiment were loaded up to $P = 25N$. The creation of permanal indentation and cracks in the ceramics are

the result of the work executed by the Vickers indenter. The microarea of Vickers diamond pyramid impressions were photographed using scanning electron microscope with magnification 500 times (Photo 1) and 1000 times (Photo 2). On both photos constant Vickers pyramid can be observed with visible edges contours inside of the impression and damage zone on the specimen surface along with many different size fragments of ceramic and radial or Palmquist cracks.[10,13,14]

Author[15] presents the table allowing to determine the degree of brittleness based on the extent of disturbance of the surface structure in the area of Vickers diamond pyramid impression. In the presented case (Plates 1 and 2) degree of brittleness is highest and equals 5.

3 INDENTATION PROCESS

The indentation process Fig. 1 consists of two steps: loading and unloading. The maximum indentation load was held constant for a few seconds before unloading. During the second phase of the experiment, the elastic alumina ceramics cause a decrease of the impression depth. After this process the total measurement depth of the impression is caused only by the permanent indentation. It was created due to the dislocation and crush of the grain in the body after the contact between the indenter and the material. Figure 2 presents the curve loading–unloading for the brittle materials.[16] The area *(Ur)* of the indentation hysteresis loop is assumed to be equal to the quantity of energy consumed by residential deformation processes.

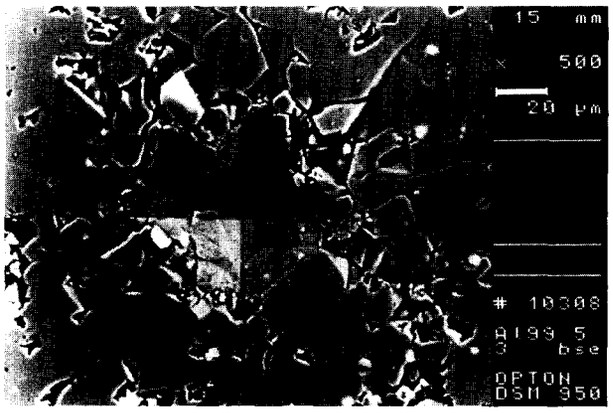

Plate 1.

Plate 2.

In the case of the ceramics material, the dependence of the value of the force on the indenter we can distinguish three kinds of indentation: (1) for the very small load (up to a few Ns)—indenter acts only on the area of one grain (usually); (2) for the average value of the load, indenter acts on a few or anywhere from 10 to 20 grains; (3) for the very high load we treat the material as isotropic and we can measure the macrohardness.

The measurement of the hardness number in all cases gives different results,[17] because the work executed during the indentation process in the monocrystal structure and in the polycrystal will be different. The microhardness is dependent on the orientation of crystallographic axis.[14] This fact influences accuracy of measurements for low loads.

In the general case of elastic-plastic deformation of the indenter the work can be written:

$$W = \int_0^h A_H h^2 dh - \int_{h_r}^h A_e (h - hr)^2 dh \qquad (2)$$

where A_H and A_e are the constants, which depend on indenter size, impression and hardness of material; h is the total depth of the indentation and is h_r is residual indentation depth (see Fig. 1).

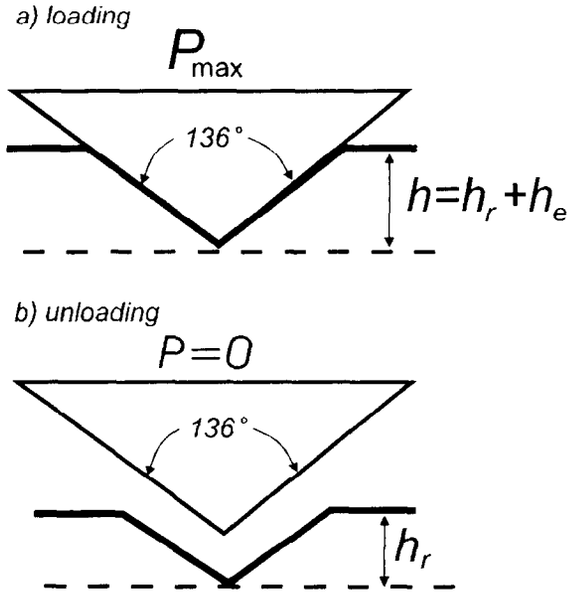

Fig. 1. The geometry of the indentation contact of a sharp indenter.

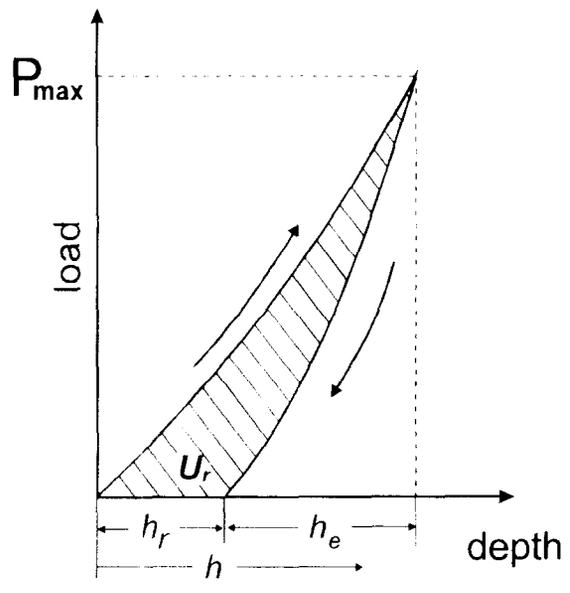

Fig. 2. The indentation hysteresis.

The work amount is the area bounded by hysteresis curve (see Fig. 2), which can be written:

$$W = w_r V \tag{3}$$

where w_r is the irreversible energy consumption to create a unit volume of indentation impression under maximum load $P_{\max}$, V is the body volume.

4 CALCULATION METHODS

Carrying out the experiment of indentation enables hardness determination, but during the experiment, crushing of the ceramics in the area of indentation takes place. In the experiment the force of pressure $P(y)$ executes a work L which is defined by

$$L = \int_o^h P(y)dy \tag{4}$$

where h is the depth of indentation and y is the direction of force operation. The dependence of the force $P(y)$ on the current depth of indentation can be found by using the definition of the Vickers hardness given by

$$H_v = \frac{P(y)}{S(y)} \tag{5}$$

where $S(y)$ is the actual area of impression in hardness testing.

The work done is equal to the critical value of elastic energy. The specific energy[6] Φ can be written as

$$\Phi = \frac{H_v}{V}\int_o^h S(y)dy \tag{6}$$

where V is the volume of the impression. Because

$$V = \int_o^h S(y)dy \tag{7}$$

eqn (6) can be written:

$$\Phi = Hv \tag{8}$$

This is a known formula that hardening is defined by necessary energy consumed to create a unit volume impression of indentation at the maximum load during elastic-plastic deformation.

On the other hand the value of the elastic energy per unit volume after transformation stress to the principal co-ordinates may be expressed as

$$\phi = \frac{(1-2v)}{6E}(\sigma_1+\sigma_2+\sigma_3)^2 + \frac{(1+v)}{6E}[(\sigma_1-\sigma_2)^2 + (\sigma_2-\sigma_3)^2 + (\sigma_3-\sigma_1)^2] \tag{9}$$

where σ_1, σ_2 and σ_3 are principal stresses, respectively, E is Young's modulus, v is Poisson's ratio. The stresses in eqn (9) are obtained during indentation for the given depth h.

In the case of predominant normal stress to the force direction, the above expression transforms to the form of

$$\phi = \frac{1}{2}\frac{\sigma_{eqv}^2}{E} \tag{10}$$

Because for the brittle and the elastic dense ceramic materials, the crushing of material does not occur in the indentation test the following condition is satisfied:

$$\phi < \Phi \tag{11}$$

In this case response of material is reversible and elastic. This condition we can present in another form, which will be used for the numerical analysis. Using eqns (8) and (10), eqn (12) takes the form:

$$\sigma_{eqv} < \sqrt{2EH_v} \tag{12}$$

The parameter σ_{eqv} used in this equation will be taken as the parameter which allows to estimate the existing state of stress after the indentation in

the brittle material (ref. Al_2O_3) or to estimate when the limit value was exceeded.

When the condition is not satisfied, then the indenter in the process of the numerical simulation moves down to the point where the parameter σ_{eqv} is satisfied.

After the larger displacement of the indenter the numerical model must be changed, because the geometry of the microstructure in the material due to motion of the sharp indenter will be changed too.

For eqn (12) crush can appear in the volume of material, and the stress state beyond the compression stress limit can be obtained from the uniaxial test.

For elastic-plastic materials this criterion is practically in the process of numerical simulation of Vickers indentation on alumina ceramics, because the equivalent stress state is estimated from the durable indentation.

The generalisation of the algorithm valid for brittle elastic materials at incremental procedure can be outlined in the following steps:

Step 1. Load the body by adding force increments ΔP. If the current force is bigger than its final value, go to Step 9.
Step 2. Calculate the body deformation.
Step 3. Calculate the stress state.
Step 4. Calculate the elastic specific energy ϕ.
Step 5. Check eqn (6): if $\sigma_{eqv} < \sqrt{2EH_v}$ then go to step 1; if $\sigma_{eqv} \geq \sqrt{2EH_v}$ then go to Step 6.
Step 6. Change the numerical model (elements in which condition $\sigma_{eqv} \geq \sqrt{2EH_v}$ is satisfied are removed from the model during the numerical simulation of Vickers indentation).
Step 7. Determine the load for the new model.
Step 8. Go back to Step 1.
Step 9. Calculate the residual stress state and the indentation parameters.

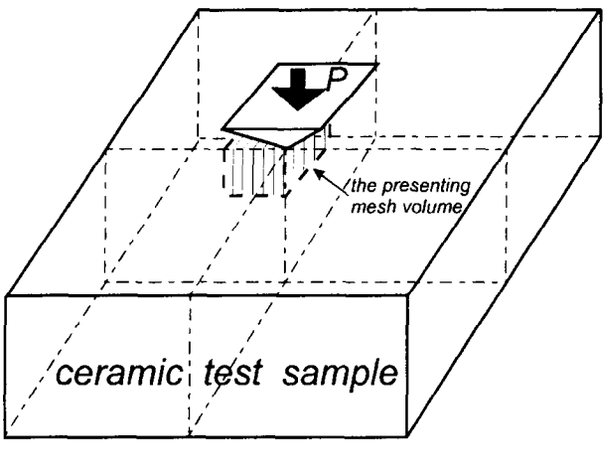

Fig. 3. The considered rectangular prism for numerical modelling.

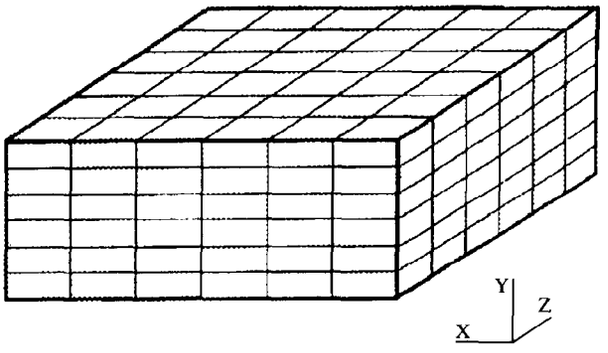

Fig. 4. Mesh of Model 1.

5 FINITE ELEMENTS METHOD MODELLING

A rectangular prism with lower surface constrained was chosen for considerations. Influence of the loading force on the centre of the upper plane of this prism was considered.

Due to the body symmetry only one-quarter of the indented microarea (Fig. 3) was used for the calculation. Three numerical models were proposed due to moving of the indenter. Model 1 (Fig. 4) which describes the beginning of the test has all the elements and the force applied to the nodes. The mesh of Model 1 (Fig. 5) has no element under the force. In this case, the depth of the indentation is equal to the length of the element on the force direction. Increment of force and nodal displacements, obtained from the calculation for

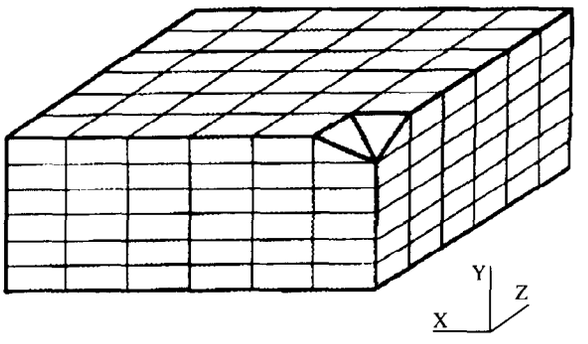

Fig. 5. Mesh of Model 2.

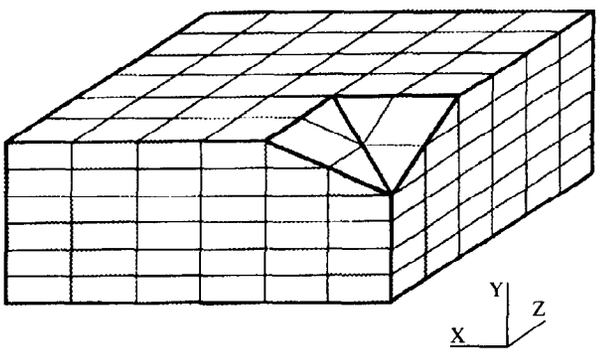

Fig. 6. Mesh of Model 3.

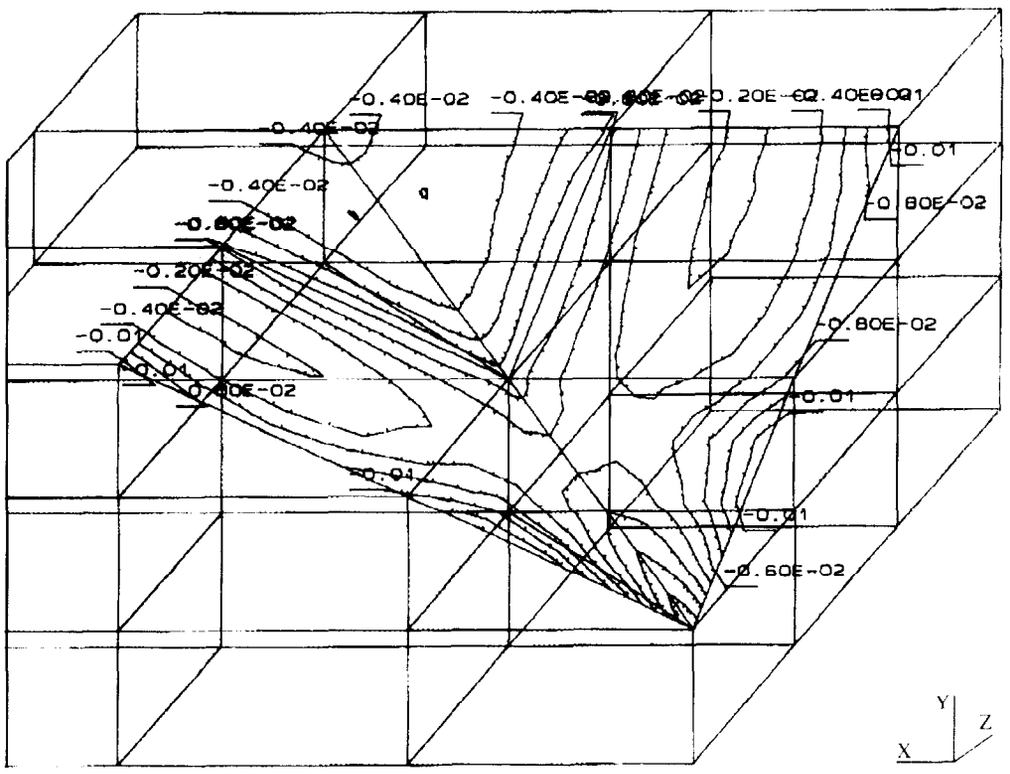

Fig. 7. Stress distribution in contact area for model 3 ($\times 10^3$ GPa).

Model 1, are the loads in the model. In Model 3 (Fig. 6) describing further displacement of the indenter, missing elements are appropriated to take the position of the indenter.

The following assumptions are taken to the numerical calculation:

- the FEM mesh of the sample was built from three-dimensional, 21-nodes finite elements, they are connected with each other at model nodes;
- in the area of trace diamonds pyramid of Vickers (apex angle 136°) was modelled;
- nodes on the following models are adjusted;
- the first stage of the load was loading of three nodes due to the blunt point (maximum dullness to 2 μm;
- the load in Model 2 was obtained from displacements in Model 1 and increment of force ΔP;
- in Model 3 the load was applied as in Model 2.

6 RESULTS AND CONCLUSIONS

The results of the calculations are presented as stress distribution of stress components in the chosen sections of models. Figure 7 presents this distribution in the area of the body in contact with the indenter for Model 3.

It is shown that the maximum stresses are in the upper area of the corner produced by the pyramid of Vickers, under the force point and in the middle sector of symmetric plane. The stresses cause all effects in the alumina ceramics (plasticity crushing, creation and propagation cracks, etc.), therefore values of these stresses are bigger than real stresses.

From this stress state can be calculated the residual stress state after the indenter removal, if the description load-depth is known for the range of loading under consideration.

From the residual stresses can be obtained directions of cracks enveloped in the volume body.

The FEM analysis of the Vickers indentation test shows its practical applicability. The presented criterion and algorithm have proven to be effective. The paper presents the first known study of Vickers indentation process by using FEM with crushing, algorithm. The FEM models were not very sophisticated. This should be expected since we have used the coarse mesh near the indentation region (lower number of degrees of freedom). The overall conclusion is that even a moderate number of finite elements employed allows to obtain quite reliable results but the computational effort must be many times bigger than in the presented case. The method proposed in the present paper can be useful in strength analysis of structures made from brittle materials under loading (results from rigid body) caused the damage in material volume. The authors of the paper will continue their work with special consideration of orthotropic effects and the influence of crystal lattice on the behaviour of the alumina ceramic during Vickers indentation process.

REFERENCES

1. RABINOVICH, V. L. & SARIN, V. K., Three-dimensional modelling of indentation fracture in brittle materials. *Mater. Sci. & Eng.*, **A206** (1996) 208–214.
2. LORCA, J. & STEINBRECH, R. W., Fracture of alumina: an experimental and numerical study. *J. Mater. Sci.*, **26** (1991) 6383–6390.
3. BATHE, K. J., *Finite Element Procedures in Engineering Analysis.* Prentice-Hall, Inc., Englewood Cliffs, NY, 1982.
4. ZIENKIEWICZ, C., *The Finite Element Method.* McGraw-Hill Book Co., London, 1977.
5. CAI, X., Finite-element method for simulation of elasto-plastic indentations by various indentors. *J. Mater. Sci. Lett.*, **11** (1992) 1527–1531.
6. LAURSEN, T. A. & SIMO, J. C., A study of the mechanics of microindentation using finite elements. *J. Mater. Res.*, **7**(3) (1992) 618–626.
7. WANG, H. F. & BANGERT, H., Three-dimensional finite element simulation of Vickers indentation on coated systems. *Mater. Sci. & Eng.*, **A163** (1993) 43–50.
8. FETT, T. & MUNZ, D., Evaluation of R-curve effects in ceramics. *J. Mater. Sci.*, **28** (1993) 742–752.
9. MARSHALL, D. B., Controlled flaws in ceramics: a comparison of Knoop and Vickers indentation. *J. Am. Ceram. Soc.*, **66**(2) (1983) 127–131.
10. BLENDELL, J. E., The origins of internal stresses in polycrystalline alumina and their effects on mechanical properties. Ph. D. thesis, Cambridge University, 1979.
11. LAWN, B. R., EVANS, A. G. & MARSHALL, D. B., Elastic/plastic indentation damage in ceramics: the median/radial crack system. *J. Am. Ceram. Soc.*, **63** (1980) 574–581.
12. BONIECKI, M. & NIEZGODA, T., *The Proceedings of the 3rd European Ceramics Society Conference*, Vol. 3, 1993, pp. 925–929,
13. MAEDA, K., NISHIOKA, H., NARITA, N. & FUJITA, S., Brittle-to-ductile transition studied by constant-rate indentation cracking. *Mater. Sci. & Eng.*, **A176** (1994) 121–126.
14. NOWAK, R. & SAKAI, M., Energy principle of indentation contact: the application to sapphire. *J. Mater. Res.*, **8**(5) (1993) 1068–1078.
15. SZYMAŃSKI, A. & SZYMAŃSKI, J. H., Hardness estimation of minerals, rocks and ceramic materials. *PWN*, (1989) Warsaw.
16. SAKAI, M., NOWAK, R., *Proceedings of the International Ceramics Conference AUSTERCERAM 92*, CSIRO Publications, Melbourne, 1992, Vol. 2, pp. 922–993.
17. BYSTRZYCKI, J. & VARIN, R. A., The frictional component in microhardness testing of intermetallics. *Scripta Metall. Mater.*, **29** (1993) 605–609.